The Voltage-gated Proton Channel Hv1 Is Required for Insulin Secretion in Pancreatic β Cells

Xudong Wang[a], Wang Xi[a], Qing Zhao[a,b], Shangrong Zhang[a], Jiwei Qin[a], Jili Lv[a], Yongzhe Che[c], Weiyan Zuo[a], Shu Jie Li[a,#]

[a]Department of Biophysics, School of Physics Science, The Key Laboratory of Bioactive Materials, Ministry of Education, Nankai University, Tianjin 300071, P. R. China

[b]Department of Cellular and Molecular Biology, School of Life Sciences, Tianjin 300071, P. R. China

[c]Department of Physiology, School of Medicine, Nankai University, Tianjin 300071, P. R. China

Running title: Loss of Hv1 inhibits insulin secretion

Address correspondence to: Dr. Shu Jie Li, Department of Biophysics, The Key Laboratory of Bioactive Materials, Ministry of Education, Nankai University, 94 Weijin Road, Nankai District, Tianjin 300071, P. R. China, Tel & Fax: +86-22-2350-6973, Email: shujieli@nankai.edu.cn

Keywords: Voltage-gated proton channel; Hv1; Pancreatic islets; β cells; Insulin secretion; Diabetes

ABSTRACT

Here, we demonstrate that the voltage-gated proton channel Hv1 represents a regulatory mechanism for insulin secretion of pancreatic islet β cell. *In vivo*, Hv1-deficient mice display hyperglycemia and glucose intolerance due to reduced insulin secretion, but normal peripheral insulin sensitivity. *In vitro*, islets of Hv1-deficient and heterozygous mice, INS-1 (832/13) cells and islets with siRNA-mediated knockdown of Hv1 exhibit a marked defect in glucose-, sulfonylurea-, K^+-, arginine-induced insulin secretion. Hv1 deficiency decreases both insulin and proinsulin contents, and has an impairment on glucose- and sulfonylurea-induced intracellular Ca^{2+} homeostasis and membrane depolarization. Furthermore, loss of Hv1 decreases insulin-containing granule pH and increases cytosolic pH in INS-1 (832/13) cells. In addition, histologic studies show a decrease in α and β cell masses in islets of Hv1-deficient mice, and a significant reduction at Hv1 expression levels in pancreatic β cells of streptozotocin (STZ)-induced diabetes mice and high-glucose induced INS-1 (832/13) cell dysfunction. Collectively, our *in vitro* and *in vivo* results indicate that Hv1 is required for insulin secretion in the β cell and a major link between β cell dysfunction and diabetes. Our study sheds light on a new biological function of the proton channel.

INTRODUCTION

Insulin secretion by pancreatic β cells is precisely regulated by glucose homeostasis. Glucose-induced insulin secretion has been proposed via two hierarchical signaling pathways (1). Glucose metabolism generates ATP and results in the closure of ATP-sensitive K^+ channels (K_{ATP} channels) and, as a consequence, the depolarization of the plasma membrane (2). This leads to Ca^{2+} influx through voltage-dependent Ca^{2+} channels and a rise in cytosolic Ca^{2+} ($[Ca^{2+}]_c$) triggering insulin exocytosis (3).

The glucose metabolism by the pancreatic β cells accompanies proton generation, which proposes a mechanism of intracellular pH-regulation behind insulin release stimulated by the sugar (4). Manipulating intracellular as well as extracellular pH could affect the insulin secretory process (4-6). Even though some studies showed that glucose

had no effect on intracellular pH (7,8), there is a large consensus that glucose induced cytosolic pH increase in mouse islets (5,9-11), rat islets (12) and insulin-secreting cell lines (13). Some studies proposed that Na^+/H^+ and Cl^-/HCO_3^- exchangers enable β cells to effectively buffer the acid load generated by glucose metabolism (9).

The pH of insulin-containing granules is between 5 and 6, which is thought to permit sequential action of pH-dependent prohormone convertases in the proteolytic processing of proinsulin and favor storage of insoluble Zn^{2+}-insulin hexamers (14,15). The acidification is carried out by a V-type H^+-ATPase that pumps H^+ into the vesicular lumen (16), and depends on Cl^- influx for charge neutralization (17). The results that glucose induces pH changes in insulin-containing granules are contradictory. Glucose slightly increased pH of secretary vesicles in normal mouse islets (18) but acidified insulin granules in RIN insulinoma cells (19). Simultaneously, other study showed that cytosolic ATP promoted granule acidification (20).

The voltage-gated proton channel Hv1 is involved in regulating intracellular pH during "respiratory burst", in which Hv1 compensates the cellular loss of electrons with protons required for NADPH oxidase (NOX)-dependent ROS generation (21,22). Clapham's group found that Hv1 contributes to brain damage in cerebral ischemia through NOX-dependent ROS generation (23). Kirichok's group successfully recorded proton current of Hv1 in human spermatozoa by patch clamp, and demonstrated that Hv1 is dedicated to inducing intracellular alkalinization and activating spermatozoa (24). Moreover, the recent studies showed that Hv1 plays important roles in breast (25,26) and colorectal (27) cancer and glioma (28) development, progression and metastasis, through regulating cancer cell intracellular pH and resulting in tumor acidic microenvironment.

Hv1 is extremely selective for protons and has no detectable permeability to other cations (29,30). Hv1 is activated by depolarization and intracellular acidification, and the gating strongly depends on both the intracellular pH (pH_i) and extracellular pH (pH_o) (29,30). Hv1 functions as a dimer and each subunit contains its own pore, in which its C-terminal domain is responsible for the protein dimeric architecture (31,32). Hv1 proton current is inhibited by submillimolar concentrations of Zn^{2+} and Cd^{2+} and other divalent

cations (21,33).

In our previous study, we have identified that Hv1 is present in human and rodent pancreatic islet β cells, as well as β cell lines (34). However, the regulatory mechanism of Hv1 for insulin secretion of pancreatic islet β cell and its relationship with β cell dysfunction and diabetes are not known. In present study, we have discovered a regulatory mechanism for the proton channel Hv1 in the modulation of β cell insulin secretory function. Our *in vitro* and *in vivo* studies demonstrate that Hv1 is required for insulin secretion in the β cell, and a major link between β cell dysfunction and diabetes.

EXPERIMENTAL PROCEDURES

Animals and treatments

Mice bearing a targeted disruption in the VSOP/Hv1 (VSOP/Hv1$^{-/-}$, backcrossed eight times) were kindly provided by Dr. Y. Okamura (School of Medicine, Osaka University), as previously described (35). WT mice (VSOP/Hv1$^{+/+}$) were of the same genetic background (C57BL/6J). Animals were kept in a pathogen-free facility under a 12-h light-dark cycle with access to water and a standard mouse diet (Lillico Biotechnology). Genotyping was performed by PCR as described by Ramsey et al. (22). Experiments were performed with 2, 4 and 6 month-old male mice, unless indicated otherwise. All animal husbandry and experiments were approved by and performed in accordance with guidelines from the Animal Research Committee of Nankai University.

Isolation of pancreatic islets

Pancreatic islets were isolated according to the collagenase digestion method described by Lacy and Kostianovsky (36), with slight modifications. Krebs-Ringer bicarbonate HEPES (KRBH) buffer (in mM: 135 NaCl, 3.6 KCl, 5 $NaHCO_3$, 0.5 NaH_2PO_4, 0.5 $MgCl_2$, 1.5 $CaCl_2$, 10 HEPES, pH 7.4) was used for islet isolation. And the isolated islets were cultured overnight in RPMI 1640 (GIBCO) containing 10% fetal bovine serum (FBS) in a humidified 5% CO_2 atmosphere at 37^{o}C before handpicking for experiments as previously described (34).

Cell culture

Pancreatic islet β cell line, INS-1 (832/13) cells were obtained from Dr. Hans Hohmeier (Duke University) and grown in RPMI 1640 medium (GIBCO) supplemented with 10% FBS, 2 mM glutamate, 1 mM sodium pyruvate and 55 μM β-mercaptoethanol in a humidified 5% CO_2 atmosphere at 37^{o}C.

siRNA silencing

To down-regulate Hv1 expression level in isolated islets and β-cells, the sequences of the small interfering RNA (siRNA) targeting the Hv1 gene 5'-CTACAAGAAATGGGAGAAT-3' and the scramble sense sequence 5'-TTCTCCGAACGTGTCACGT-3', which were obtained from Ribobio (Guangzhou, China), were used, as described previously (34).

Quantitative real-time PCR

The mRNA expression levels of insulin in isolated islets and INS-1 (832/13) cells, were evaluated by quantitative real-time PCR using ABI PRISM 7000 Sequence Detection System (Applied Biosystems, Foster City, CA), as described previously (34). The primers were as follows: insulin, 5'- CCTCACCTGGTGGAGGCTC-3' (forward) and 5'-ACAATGCCACGCTTCTGC-3' (reverse); GAPDH, 5'-CCAAGGTCATCCATGACAAC-3' (forward) and 5'-AGAGGCAGGGATGATGTTCT-3' (reverse). All experiments were performed in triplicate.

Insulin secretion assay

Insulin secretion from isolated islets and INS-1 (832/13) cells was measured as previously described (34). Total insulin and proinsulin content in isolated islets and INS-1 (832/13) cells were extracted with acidic ethanol and determined using rat/mouse proinsulin, mouse and rat insulin ELISA (Mercodia, Uppsala), according to the manufacturer's protocol.

Blood glucose and insulin determinations

Blood glucose levels were measured from blood obtained from the tail vein after fasting 6 h using an automated glucometer (One Touch, Johnson & Johnson, USA). For glucose tolerance tests, mice at 2, 4 and 6 months of age were fasted for 6 h before

intraperitoneal (i.p.) injection with glucose (2 g/kg body weight), and blood glucose concentration was measured at 0, 15, 30, 60 and 120 min after the injection. For insulin tolerance tests, mice were fasted for 6 h before intraperitoneal injection with insulin (1.0 units/kg body weight), and blood glucose concentration was measured at 0, 15, 30, 60 and 120 min.

For serum insulin measurements, glucose (2 g/kg body weight) or L-arginine (1 g/kg body weight) was injected i.p., and venous blood was collected at 0, 2, 5, 15, and 30 min in chilled heparinized tubes, immediately centrifuged, and the serum stored at -80^{o}C. Insulin levels were measured by ELISA (Mercodia, Uppsala).

Islet cAMP content

Islets in groups of 50 were preincubated for 1 h at 2.8 mM glucose in KRBH/BSA, and then stimulated with 16.7 mM glucose in the presence of 10 μM forskolin for 30 min at 37 ℃. After the supernatants were removed, the islets were washed once with ice-cold KRBH, and then ice-cold HCl (100 μl, 0.1 mM) was added to islet pellets followed by 10 min agitation at 4 ℃. After neutralization with 100 μl 0.1 mM NaOH, islet cAMP contents were determined using an Enzyme Immunoassay kit (Sigma-Aldrich, St Louis, MO) according to the manufacturer's protocol.

Measurements of intracellular Ca^{2+}

Cellular Ca^{2+} changes were monitored as previously described (34).

Measurements of membrane potential

The voltage-sensitive bis-oxonol fluorescent dye $DiBAC_4(3)$ was used to study the membrane potential changes of INS-1 (832/13) β cells. The β cells transfected with the scramble or Hv1-targeting siRNA were incubated with 2 μM $DiBAC_4(3)$ for 10 min at 37 ℃ in a solution (in mM: 138 NaCl, 5.6 KCl, 1.2 $MgCl_2$, 2.6 $CaCl_2$, 2.8 glucose and 10 HEPES, pH 7.4) prior to fluorescence measurement. Data were expressed as an average of five experiments (50-80 cells per experiment).

Measurements of intragranular pH

Intraluminal pH of insulin granules was monitored semi-quantitatively by fluorescent probe LysoSensor-Green DND-189 (LSG) (Invitrogen). LSG accumulates in acidic

organelles and exhibits a pH-dependent fluorescence (20). INS-1 (832/13) cells were loaded with 1 μM LSG for 30 min at 37°C in a buffer (in mM: 140 NaCl, 5 KCl, 1 $MgSO_4$, 1 $CaCl_2$, 1 NaH_2PO_4, 2.8 glucose, and 10 HEPES, pH 7.4), and the fluorescence of LSG was detected at 488 nm excitation and 510 nm emission. All LSG experiments were performed at 20 ℃ to prevent exocytosis, which excludes the possibility of an artefactual decrease in measured granular pH caused by cell swelling during exocytosis (37). The data were normalized to control and expressed as an average of five experiments (50-80 INS-1 (832/13) cells per experiment).

Measurements of cytosolic pH

Cytosolic pH was measured using BCECF fluorescence, as described previously (26). INS-1 (832/13) cells were loaded with 3.0 μM of BCECF-AM (Molecular Probe) in FBS-free RPMI 1640 medium at 37°C for 30 min, and then washed and loaded in a buffer (in mM: 140 NaCl, 5 KCl, 1 $MgSO_4$, 1 $CaCl_2$, 1 NaH_2PO_4, 2.8 glucose, and 10 HEPES, pH 7.4) for measurements. The data was expressed as an average of five experiments (50-80 INS-1 (832/13) cells per experiment).

Immunohistochemistry

Immunohistochemistry was performed as described previously (34).

Streptozotocin (STZ) diabetes model

To induce diabetes, WT and $Hv1^{-/-}$ mice were treated with STZ (50 mg/kg body weight i.p. for 5 consecutive days). Additionally, some WT and $Hv1^{-/-}$ mice were treated with saline as vehicle controls. Blood glucose levels were measured once every week with fasting 6 h after the final injection of STZ. At the end of the forth week, an i.p. glucose tolerance test (IPGTT) was performed using an i.p. injection of glucose at 2 g/kg body weight after 6 h fasting. Blood glucose was analyzed at 0, 15, 30, 60, and 120 min after introducing glucose. Diabetic hyperglycemia was defined as a fasting blood glucose concentration ＞ 11.1 mM for two or more consecutive tests.

Statistical analysis

All statistics were performed using SPSS20.0 software. Measurement data were represented as mean ± SEM. Comparison of the mean between groups was performed by *t*

test. *P* values < 0.05 were considered significant.

RESULTS

Reduced insulin secretion of islets from Hv1-deficient mice

To delineate the role of Hv1 in insulin secretion, we performed insulin secretion assays using isolated islets from wild type (WT, $Hv1^{+/+}$), heterozygous ($Hv1^{+/-}$) and homozygous (KO, $Hv1^{-/-}$) mice. As shown in Fig. 1A, 16.7 mM glucose-induced insulin secretion was greatly reduced by 51 (n = 8, $p < 0.001$) and 78% (n = 8, $p < 0.001$) in heterozygous and KO islets compared with WT islets (n = 8). While, basal insulin secretion (at 2.8 mM glucose) in heterozygous and KO islets was also significantly reduced by 60 (n = 8, $p < 0.001$) and 80% (n = 8, $p < 0.001$) compared with WT islets (n = 8). Similar results were observed for tolbutamide- and glibenclamide-induced insulin secretion in heterozygous and KO islets, which were significantly reduced by 78 (n = 8, $p < 0.001$) and 85% (n = 8, $p < 0.001$), 61 (n = 8, $p < 0.001$) and 67% (n = 8, $p < 0.001$), for heterozygous and KO islets, respectively, compared with WT islets (n = 8) (Fig. 1A). Direct depolarization elicited by an increase of extracellular K^+ (60 mM KCl) also attenuated insulin secretion by 59 (n = 8, $p < 0.001$) and 65% (n = 8, $p < 0.001$) in heterozygous and KO islets compared with WT islets (n = 8) (Fig. 1A), indicating that knockout of Hv1 prevents K^+-induced insulin secretion in pancreatic β cells. Furthermore, arginine-induced insulin secretion of islets from heterozygous and KO mice was decreased by 67 (n = 8, $p < 0.001$) and 89% (n = 8, $p < 0.001$) compared with WT islets (n = 8) (Fig. 1A), as seen *in vivo*. Together, these data indicate that loss of Hv1 in islets inhibits insulin secretion.

Insulin and proinsulin contents in KO islets were reduced by 17 (n = 8, $p < 0.001$) and 25% (n = 8, $p < 0.01$), respectively, compared with WT islets (n = 8) at a basal condition (2.8 mM glucose) (Fig. 1B and C). The ratio of insulin to proinsulin content, however, was indistinguishable between KO and WT islets (Fig. 1D), suggesting that insulin synthesis is abnormal, but not insulin maturation in Hv1-deficient islets. The proinsulin secretion was barely detectable under basal conditions (2.8 mM glucose) in WT,

heterozygous and KO islets (data not shown). In the presence of 16.7 mM glucose, the proinsulin secretion was reduced by 59 (n = 8, $p < 0.001$) and 78% (n = 8, $p < 0.001$) in heterozygous and KO islets, compared with WT islets (n = 8) (Fig. 1E). However, the ratios of insulin to proinsulin secretion in heterozygous and KO islets in the presence of 16.7 mM glucose were not different with WT islets (Fig. 1F), suggesting that no significant accumulation of proinsulin occurred in KO islets.

Knockdown of Hv1 inhibits secretagogue-induced insulin secretion

To further examine the effect of Hv1 on insulin secretion, we used RNA interference to instantaneously reduce endogenous Hv1 levels in INS-1 (832/13) cells and isolated islets. The insulin secretion of INS-1 (832/13) cells and the islets at a basal condition (2.8 mM glucose) was low at both the controls and Hv1-knockdown INS-1 (832/13) cells and islets (Fig. 2A and Fig. S1). In the presence of 16.7 mM glucose, 200 μM tolbutamide and 1 μM glibenclamide, the insulin secretion in the control INS-1 (832/13) cells increased 9.6, 10.3 and 8.2-fold compared with that at the basal condition, respectively. Whereas the insulin secretion was significantly reduced by 64 ($p < 0.001$), 60 ($p < 0.001$) and 73% ($p < 0.001$) by a reduction in Hv1 level with Hv1-targeting siRNA, respectively (Fig. 2A), indicating that Hv1 markedly affects the glucose- and sulfonylurea-induced insulin secretion in INS-1 (832/13) cells. In accordance with the INS-1 (832/13) cells, the insulin secretion was reduced by 57 ($p < 0.001$), 48 ($p < 0.001$) and 57% ($p < 0.001$) in the Hv1-downregulated isolated islets compared with the controls at 16.7 mM glucose, 200 μM tolbutamide and 1 μM glibenclamide, respectively (Fig. S1).

To examine the effect of Hv1 on insulin processing, the insulin and proinsulin contents were measured. At a basal condition (2.8 mM glucose), the contents of both insulin and proinsulin were reduced by 36 ($p < 0.001$) and 39% ($p < 0.001$) respectively, in the Hv1-silenced INS-1 (832/13) cells, compared with the controls (Fig. 2B and C). In comparison to the INS-1 (832/13) cells, the contents of insulin and proinsulin were decreased by 42 ($p < 0.001$) and 40% ($p < 0.001$), respectively, in the Hv1-downregulated islets (Fig. S2, A and B). However, the ratio of insulin to proinsulin content has a no

difference between the controls and the Hv1-downregulated INS-1 (832/13) cells (Fig. 2D) and islets (Fig. S2, C), demonstrating that Hv1 has an impact on proinsulin synthesis. To further verify the effect of Hv1 on insulin synthesis, the insulin mRNA expression levels in the INS-1 (832/13) cells and the isolated islets were measured. As shown in Fig 2E and F, insulin mRNA level was decreased by 38 ($p < 0.01$) and 33% ($p < 0.01$) by a reduction in Hv1 level with Hv1-targeting siRNA in the INS-1 (832/13) cells and islets, respectively, compared with the controls, indicating that knockdown of Hv1 has an effect on insulin synthesis.

To detect the effect of Hv1 on proinsulin secretion, we then measured the proinsulin secretion in the INS-1 (832/13) cells and isolated islets. The proinsulin secretion was barely detectable under basal conditions in both control and Hv1-silenced islets, but in the presence of 16.7 mM glucose, the proinsulin secretion was reduced by 68 ($p < 0.01$) and 63% ($p < 0.001$) by a reduction in Hv1 level, compared with the controls, in the INS-1 (832/13) cells and islets, respectively (Fig. 2G; Fig. S3, A). However, the ratio of insulin to proinsulin secretion in Hv1-silenced INS-1 (832/13) cells and islets in the presence of 16.7 mM glucose was not different with that in control INS-1 (832/13) cells and islets (Fig. 2H; Fig. S3, B), suggesting that no significant accumulation of proinsulin occurred in the Hv1-silenced INS-1 (832/13) cells and islets.

Hv1-deficient mice exhibit hyperglycaemia and impaired glucose tolerance due to reduced insulin secretion

To assess the effect of Hv1 knockout on glucose homeostasis, glucose levels were measured in 4 month-old mice in fasted state. The body weight curves of the control (WT, $Hv1^{+/+}$), heterozygous ($Hv1^{+/-}$) and homozygous (KO, $Hv1^{-/-}$) littermates were almost similar (Fig. 3A), but the blood glucose levels in fasted state were markedly higher in heterozygous (9.3 ± 0.4 mmol/l, n = 24, $p < 0.001$) and KO (10.2 ± 0.6 mmol/l, n = 24, $p < 0.001$) mice compared with WT mice (6.2 ± 0.2 mmol/l, n = 24) (Fig. 3B).

To evaluate the impact of Hv1 on disposal of a glucose load, intraperitoneal (i.p.) glucose tolerance tests (IPGTT) were performed. Compared with WT mice, both KO and

heterozygous mice in 4 months of age showed significantly higher glucose levels following an i.p. glucose load (2 g/kg body weight) (Fig. 3C). Corresponding serum insulin levels (including basal) were lower in both KO and heterozygous mice throughout the IPGTT after the glucose challenge compared with WT mice, providing evidence for an insulin secretion defect in response to glucose (Fig. 3D). Interestingly, KO and heterozygous mice exhibited a selective loss of acute first-phase insulin secretion in response to glucose (Fig. 3D). The insulin levels, however, did a little gradually rise after the glucose challenge, suggesting some retention of second-phase insulin secretion in both KO and heterozygous mice (Fig. 3D). Thus, the Hv1KO mice exhibit an impairment in their ability to dispose of a glucose load due to insulin secretion defect.

To further evaluate the effect of Hv1 deletion on insulin secretion *in vivo*, insulin secretion in response to stimulation with arginine the major nutrient secretagogue of insulin was measured. The mechanisms of arginine-stimulated insulin secretion is independent on those by glucose, although the final pathways of secretion are the same (38). Therefore, to determine the level of defect in glucose-stimulated insulin secretion, mice were also given an arginine challenge. As shown in Fig. 3E, serum insulin levels (including basal) were significantly lower in KO mice after the arginine injection (1 g/kg body weight) compared with WT mice. In contrast to the response to glucose, in both KO and heterozygous mice in 2 and 4 months of age, there was a first-phase insulin release in response to arginine (Fig. 3E).

To explore the possibility that the observed glucose intolerance was the result of peripheral insulin resistance, we performed i.p. insulin tolerance tests (IPITT) in Hv1KO mice in 2 and 4 months of age. We found that insulin administration lowered blood glucose levels in both WT and Hv1-deficient mice to a similar extent, indicating that Hv1 deficiency does not impair a peripheral insulin sensitivity (Fig. 3F). Taken Together, these data are compatible with the notion that loss of Hv1 results in impaired glucose tolerance due to a defect of insulin secretion *in vivo*.

Knockdown of Hv1 has no effect on cAMP generation

cAMP is an important second messenger involved in potentiating rather than initiating insulin secretion (39). To detect the effect of Hv1 on cAMP production, we measured forskolin enhanced insulin secretion and cAMP content in isolated islets. In the present of 10 μM forskolin, at 2.8 mM glucose, the insulin secretion in Hv1-silenced islets was decreased by 37% ($p < 0.01$) compared with that in control islets, while at 16.7 mM glucose, the insulin secretion was reduced by 63% ($p < 0.001$) (Fig. 4A). The cAMP content in Hv1-silenced islets was not different with that in control islets in the present of 10 μM forskolin and 16.7 mM glucose (Fig. 4B), suggesting that knockdown of Hv1 has no effect on cAMP production.

Glucagon-like peptide-1 (GLP-1) is an intestinally derived insulinotropic hormone, which increases cAMP generation and results in insulin release (40). To further confirm the effect of Hv1 on cAMP production, we examined GLP-1-stimulated insulin secretion in Hv1-silenced INS-1 (832/13) cells. At 16.7 mM glucose, 10 and 100 nM GLP-1 stimulated insulin secretion 2.3 and 2.7-fold over without GLP-1 (16.7 mM glucose) (Fig. 4C). However, the insulin secretion from the Hv1-silenced cells was decreased by 73 ($p < 0.001$) and 53% ($p < 0.001$) in the presences of 10 and 100 nM GLP-1, respectively, compared with the control (Fig. 4C), indicating that the effect of Hv1 on insulin secretion is independent on cAMP pathway.

Deficiency of Hv1 impairs cellular Ca^{2+} homeostasis and membrane depolarization

Glucose stimulates insulin secretion by induction of Ca^{2+}-dependent electrical activity that triggers exocytosis of the insulin granules. We found that siRNA-mediated knockdown of Hv1 in INS-1 (832/13) cells impaired tolbutamide-induced intracellular Ca^{2+} homeostasis (Fig. 5A and B). Zn^{2+} is a classical inhibitor of Hv1 (29,41). 10 μM Zn^{2+} can efficiently inhibit Ca^{2+} influx stimulated by 200 μM tolbutamide (Fig. 5C). In pancreatic β cells, the increase of cytosolic Ca^{2+} ($[Ca^{2+}]c$) occurs with Ca^{2+} entry across voltage-sensitive Ca^{2+} channels activated by membrane depolarization (3). To confirm whether the abrogation of Ca^{2+} influx by suppression of Hv1 is coupled to membrane polarization, the membrane potential changes of INS-1 (832/13) cells during glucose- and

tolbutamide-stimulation were monitored with $DiBAC_4(3)$ fluorescence. As shown in Fig. 5D and E, the control cells were depolarized significantly more than Hv1-silenced INS-1 (832/13) cells after glucose or tolbutamide stimulation, indicating that Hv1 deficiency impairs glucose or tolbutamide-induced membrane depolarization. Thus, the reduction in insulin secretion by deficiency of Hv1 must therefore involve in electrical activity and $[Ca^{2+}]c$ signaling.

Knockdown of Hv1 acidifies intragranules and alkalizes cytosol

Our previous results showed that Hv1 is expressed in insulin-containing granules (34). To assess the effect of Hv1 on insulin granule pH, the intragranule pH was monitored by LysoSensorGreen DND-189 (LSG) fluorescence. LSG accumulates in acidic organelles and exhibits a pH-dependent fluorescence: its fluorescence increases with a pH decrease, but no fluorescence in alkalinization (37). We found that the LGS fluorescence in Hv1-deleted INS-1 (832/13) cells was increased compared with that in the control cells, indicating that the intragranules in the Hv1-deleted cells were acidified (Fig. 5F). These observations indicated that knockdown of Hv1 inhibits Hv1-mediated proton extrusion and acidifies insulin-containing granules. Therefore, Hv1 involves in intragranule pH regulation in pancreatic β cells.

To evaluate the effect of Hv1 on cytosol pH (pH_c), the pH_c of INS-1 (832/13) cells was measured by BCECF fluorescence. As shown in Fig. 5G, the pH_c in the cells treated with scramble sequence was 7.17 ± 0.04, but the pH_c was increased to 7.28 ± 0.04 in the cells treated with Hv1-targeting sequence, indicating that the down-regulation of Hv1 expression in INS-1 (832/13) cells obviously alkalizes cytosol. These results demonstrated that inhibition of Hv1-mediated proton extrusion from intragranules alkalizes cytosol in the β cell.

Deficiency of Hv1 reduces α and β cell masses and pancreatic insulin content

To determine whether Hv1 deletion affects islet development, we conducted immunohistologic (IHC) studies. Morphometric analysis of pancreatic sections from WT,

heterozygous and KO mice at 4 months of age exhibited a relatively normal islet architecture in each case, with β cells concentrated in the core and α cells located mainly in the periphery (Fig. 6A), while the morphology of isolated islets cultured overnight from KO mice is not overtly different from WT islets (data not shown). On the other hand, the number of the isolated islets per pancreas is not significantly different between WT and KO mice (data not shown) , which is consistent with the result from immunohistochemical analysis (Fig. 6B). However, the islet average size calculated from isolated islets (Fig. 6C) and islet area to total pancreas area (Fig. 6D) analyzed by immunohistochemistry of pancreatic sections were decreased in the KO mice compared with WT and heterozygous mice.

Interestingly, quantification of total α and β cell masses displayed a genotype-dependent difference. α and β cell masses were decreased by 71 (n = 6, $p < 0.01$) and 13% (n = 6, $p < 0.05$) in Hv1KO mice compared with WT mice (n = 6), respectively, as measured by morphometric analyses of insulin and glucagon positive islet cells (Fig. 6E and F). The total pancreatic insulin content in Hv1KO mice was also decreased by 11% (n = 6, $p < 0.05$) (Fig. 6G), the same as the observed in the isolated islets (Fig. 1B). These results show that Hv1KO mice have sufficient β cells and insulin, indicating that the *in vivo* phenotype is not due to a gross developmental defects.

Hv1-deficient mice exhibits an age-dependent development in glucose intolerance and a decrease in β cell mass

To further estimate the effects of Hv1 on glucose tolerance, we performed IPGTT of the 2 and 6 month-old WT and Hv1KO mice as described above. The 6 month-old KO mice showed more serious glucose intolerance than the 2 month-old KO mice (Fig. 7A), while the WT mice showed no glucose intolerance in different ages. Then we performed the IPITT and tested the serum insulin levels in response to glucose and arginine of the 2 and 6 month-old WT and Hv1KO mice, which showed no significant differences in age in both WT and KO mice (Fig. 7B, C and D).

Consistent with the above, the β cell mass of 6 month-old Hv1KO mice was

decreased by 43% (n = 6, $p < 0.05$) (Fig. 7E) compared with 6 month-old WT mice, while there was no significant difference between 2 month-old Hv1KO and WT mice in β cell mass. The age-dependent decrease of β cell mass might be the reason of more serious glucose intolerance in older Hv1-deficient mice.

Hv1 is down-regulated in pancreatic β cells in STZ-induced diabetic mice

To further determine the relationship between Hv1 and insulin secretion, the WT and Hv1KO mice were treated with STZ to induce diabetes. We found the fasted blood glucose levels after the STZ injection in Hv1KO mice were always higher than WT mice (Fig. 9A), and the IPGTT also showed higher blood glucose levels in STZ-treated Hv1KO mice than WT mice (Fig. 8B). These data shows that STZ-treated Hv1KO mice seem more sensitive to be induced to diabetes.

The insulin content at 2.8 mM glucose was decreased by 91% in β cells of STZ-treated WT mice (Fig. 8C), while the insulin secretion stimulated by 16.7 mM glucose was reduced by 97% (Fig. 8D), which showed a serious insulin deficiency. The immunohistochemical analyses of islets in control and STZ-treated WT mice using anti-insulin and anti-Hv1 antibodies also showed the mean optic density of insulin- and Hv1-positive area in STZ-treated WT mice were decreased by 53% and 60% compared to control mice, respectively (Fig. 8E), demonstrating that the expression levels of both insulin and Hv1 are significantly decreased in β cells of STZ-treated diabetes mice, as shown in Fig 9E, b and d. The lower expression of Hv1 in the β cell in the diabetes mice might be due to the decrease in insulin secretion, which is consistent with the result that the insulin secretion is significantly reduced in islets of $Hv1^{+/-}$ mice (Fig. 1A). These data suggests that the Hv1 is closely related to insulin secretion.

Hv1 is down-regulated in high glucose-induced dysfunctional β cells

Chronic hyperglycemia can cause loss of glucose-stimulated insulin secretion (GSIS) (42). To confirm whether Hv1 is also down-regulated in dysfunctional β cells, INS-1 (832/13) cells were incubated in 11 and 25 mM glucose for 48 h, respectively. Following

chronic incubation, insulin secretion were measured at two different concentrations of glucose (2.8 and 16.7 mM), and Hv1 expression levels were detected by immunofluorescence.

Insulin secretion in INS-1 (832/13) cells incubated chronically at 11 mM glucose was increased in response to glucose stimulation, but completely unresponsive in 25 mM glucose chronic incubation (Fig. 9A). These data are consistent with other report (42) showing that chronic high glucose causes complete loss of glucose responsiveness in INS-1 (832/13) cells. The immunofluorescence analyses of the cells at 11 and 25 mM glucose chronic incubation using anti-Hv1 antibody showed the mean fluorescence intensity in 25 mM glucose chronic incubation cells was decreased by 33.5% compared to 11 mM (Fig. 9B). These data demonstrated that Hv1 expression level is also significantly decreased in the dysfunctional β cells, which is in accordance with that in STZ-induced diabetes model.

DISCUSSION

Here, we show *in vivo*, that both Hv1KO and heterozygous mice display hyperglycemia and glucose intolerance due to markedly decreased insulin secretion. *In vitro*, deficiency of Hv1 exhibits a remarkable defect in secretagogue-induced insulin secretion, decreases both insulin and proinsulin contents, impairs intracellular Ca^{2+} homeostasis and membrane depolarization, decreases insulin-containing granule pH and increases cytosolic pH. Interestingly, a decrease in α and β cell masses in Hv1KO mice has been observed, especially α cell mass. These data indicate that the level of Hv1 expression in the β cell is required for insulin secretion and maintaining glucose homeostasis, and reveal a significant role for the proton channel in the modulation of pancreatic β cell function.

Vacuolar H^+-ATPases deliver protons to organellar lumen, generating an electrical potential (inside positive) across the organellar membrane that antagonize further inward transport of protons (16). K^+ and Cl^- are favored candidates as counterions to compensate the electrogenic displacement of protons by the V-ATPases (20,43). The theoretical

maximal luminal pH generated by the V-ATPases is less than 3, calculated on a thermodynamic basis (16). That is clearly much more acidic than insulin-containing granular pH (5-6) determined experimentally (14,15), suggesting the existence of a proton (equivalent) back-flux or "leak". Demaurex et al. (44) found that the leakage of protons from the Golgi is exquisitely voltage and pH sensitive, and could be reduced by addition of micromolar concentrations of Zn^{2+}. By analogy with Zn^{2+}-sensitive pathways described at the plasmalemma, these authors suggested that proton-conductive channels may exist in the membranes of secretory organelles. Schapiro and Grinstein (45) also found that the channel for Golgi proton leak has a high temperature coefficient. Our previous work demonstrates that Hv1 localizes to insulin-containing granule membrane (34). Knockdown of Hv1 results in a decrease in the insulin-containing granular pH (intragranule acidification) and an increase in cytosol, indicating that Hv1 is involved in regulating insulin-containing granular pH. Considering that Hv1 channel is activated at depolarizing voltages, sensitive to the membrane pH gradient, H^+-selective, Zn^{2+}- and temperature-sensitive, therefore, Hv1 is responsible for the proton "leak" in insulin-containing granules.

The acidification inside the secretory vesicles has a fundamental importance for maintenance of whole-body homeostasis. It has been suggested for decades that the proton gradients might be involved in the fusion of secretory vesicles to the target membrane (46,47). Barg et al. (20) showed that the acidic pH might regulate priming of the granules for secretion, a process involving pairing of SNARE proteins on the vesicles and target membranes to establish fusion competence. The dependence of the insulin secretion on Hv1 activity reflects that the intragranule pH is directly involved in the secretion of secretory granules. We presumed that loss of Hv1 would result in abnormal luminal acidification, and thereby affect insulin synthesis and maturation.

Glucose metabolism generates ATP and closes ATP-regulated K^+ channels, leading to membrane depolarization. The membrane depolarization of the β cell leads to activation of voltage-sensitive L-type Ca^{2+} channels, with a subsequent rise of intracellular Ca^{2+}, which then drives vesicular exocytosis (48). cAMP is an important intracellular massager for potentiation of glucose-stimulated insulin secretion (49) and proposed to influence

insulin secretion at multiple steps (50). cAMP action in insulin secretion is well known to be mediated via two distinct pathways, one mediated by protein kinase A (PKA) and the other by PKA-independent mechanisms involving the cAMP binding protein Epac2 (49,51). cAMP-dependent steps also require adequate intracellular ATP, the enzyme adenylate cyclase catalyzes the conversion of ATP to cAMP (39,49 48). In the present work, knockdown of Hv1 has no effect on cAMP production, suggesting that Hv1 does not influence the ATP generation.

Sulfonylureas such as tolbutamide and glibenclamide, bind to the SUR subunit of the ATP-sensitive K^+ channels and induce channel closure (52). We demonstrate that the lack of Hv1 inhibits sulfonylurea-induced insulin secretion, indicating that the effect of Hv1 on insulin secretion is not related to the ATP-sensitive K^+ channel pathway. We also show that ablation of the Hv1 gene abolishes the entry of calcium ions into the β cell evoked by glucose or tolbutamide. This important defect could be predicted from the reduced depolarization that we observed in the β cell. This indicates that β cells lacking Hv1 proton channel cannot generate Ca^{2+} influx when membrane cannot be depolarized. The fact that heterozygous mice also have a hyperglycemia with a low insulin level illustrates that Hv1 is at an important control point in the metabolic pathway regulating insulin secretion, and that relatively small changes in Hv1 activity are likely to have important effects on insulin secretion. Similar effects have been observed for glucokinase (53). The findings of the present study clearly demonstrate that Hv1 plays an important role in positively regulating secretagogue-stimulated insulin secretion.

β cell failure is associated with not only decreased β cell insulin secretory function but also reduced overall β cell mass (54). In present study, there was no difference in islet morphology between Hv1KO and WT mice, and only a very modest decrease in islet size and β cell mass, but a significant decrease in α cell mass. The smaller size observed in Hv1-deficient pancreatic islets may be related to the decrease in α and β cell masses, and result from impaired insulin secretory function. In this context, it is important to note that *in vitro* siRNA-mediated knockdown of Hv1 in isolated islets and INS-1 (832/13) β cells caused decreased glucose-stimulated insulin secretion (GSIS), suggesting that the *in vivo*

decrease in insulin secretion in the Hv1KO mice was not due to an *in vivo* β cell developmental defect.

Taken together, the data in the present study demonstrate that Hv1-deficient mice exhibit a hyperglycemia and impaired glucose tolerance due to reduced insulin secretion. The finding provides direct evidence of a functional role for the proton channel in the maintenance of glucose homeostasis. These studies describe a novel pathway regulating β cell secretory function in which Hv1 sustains the entry of calcium ions into β cell through regulating membrane depolarization to promote increased insulin secretory responses. Considering that Hv1 is a positive regulator of insulin secretion and that relatively small changes in Hv1 levels significantly impact on insulin secretion, we hypothesized that decreased Hv1 expression might be associated with type 2 diabetes.

Acknowledgements

We would like to thank Dr. Y. Okamura (School of Medicine, Osaka University) for providing VSOP/Hv1 KO mice. We would like to thank Dr. Hans E. Hohmeier (Duke University Medical Center) for providing materials mentioned in the text. This work was supported by National Natural Science Foundation of China (No. 30970579 and 31271464), the Ph.D. Programs Foundation of Ministry of Education of China (No. 20110031110004 and 20120031110028), and the Basic Science and Advance Technology Research Program of Tianjin (No. 14JCYBJC23400).

Conflict of interest

The authors declare that they have no conflict of interest.

Author contributions

SJL and XDW conceived and designed the study. XDW, WX, QZ, SRZ, JWQ, JLL, YZC, WYZ and SJL performed the experiments. SJL and XDW wrote the paper. SJL and XDW reviewed and edited the manuscript. All authors were involved in data analysis, read and approved the manuscript.

References

1. Henquin, J.C., M.A. Ravier, M. Nenquin, J.C. Jonas, and P. Gilon. Hierarchy of the β-cell signals controlling insulin secretion. *Eur. J. Clin. Invest.* 33:742–750 (2003).
2. Aguilar-Bryan, L., and J. Bryan. Molecular biology of adenosine triphosphate-sensitive potassium channels. *Endocr. Rev.* 20:101–135 (1999).
3. Rorsman, P., and E. Renstrom. Insulin granule dynamics in pancreatic beta cells. *Diabetologia* 46:1029–1045 (2003).
4. Pace, C.S., J.T. Tarvin, and J.S. Smith. Stimulus-secretion coupling in beta-cells: modulation by pH. *Am. J. Physiol.* 244: E3-18 (1983).
5. Lindström, P., and J. Sehlin. Effect of glucose on the intracellular pH of pancreatic islet cells. *Biochem. J.* 218:887-892 (1984).
6. Lindström P., and J. Sehlin. Effect of intracellular alkalinization on pancreatic islet calcium uptake and insulin secretion. *Biochem. J.* 239:199-204 (1986).
7. Hellman, B., J. Sehlin, and I.B. Taljedal. The intiacellular pH of mammalian pancreatic beta-cells. *Endocrinology* 90:335-337 (1972).
8. Grapengiesser, E., E. Gylfe, and B. Hellman. Regulation of pH in individual pancreatic ß-cells as evaluated by fluorescence ratio microscopy. *Biochim. Biophys. Acta* 1014:219-224 (1989).
9. Juntti-Berggren, L., P. Arkhammar, T. Nilsson, P. Rorsman, and P.O. Berggren. Glucose-induced increase in cytoplasmic pH in pancreatic beta-cells is mediated by Na^+/H^+ exchange, an effect not dependent on protein kinase C. *J. Biol. Chem.* 266:23537–23541 (1991).
10. Shepherd, R.M., and J.C. Henquin. The role of metabolism, cytoplasmic Ca^{2+}, and pH-regulating exchangers in glucose-induced rise of cytoplasmic pH in normal mouse pancreatic islets. *J. Biol. Chem.* 270:7915–7921 (1995).
11. Salgado, A., A.M. Silva, R.M. Santos, and L.M. Rosario. Multiphasic action of glucose and α-ketoisocaproic acid on the cytosolic pH of Pancreatic β-Cells evidence for an acidification pathway linked to the stimulation of Ca^{2+} influx. *J. Biol. Chem.* 271:8738–8746 (1996).

12. Lebrun, P., E.V. Ganse, M. Juvent, M. Deleers, and A. Herchuelz. Na^+-H^+ exchange in the process of glucose-induced insulin release from the pancreatic B-cell. Effects of amiloride on ^{86}Rb,^{45}Ca fluxes and insulin release. *Biochim. Biophys. Acta* 886:448–456 (1986).
13. Lynch, A.M., J.E. Meats, L. Best, and S. Tomlinson. Effect of extracellular sodium removal upon ^{86}Rb outflow from pancreatic islet cells. *Biochim. Biophys. Acta* 1012:166–170 (1989).
14. Orci, L., M. Ravazzola, M. Amherdt, O. Madsen, A. Perrelet, J.D. Vassalli, and R.G. Anderson. Conversion of proinsulin to insulin occurs coordinately with acidification of maturing secretory vesicles. *J. Cell Biol.* 103:2273–2281 (1986).
15. Hutton, J.C. The insulin secretory granule. *Diabetologia* 32:271–281 (1989).
16. Paroutis, P., N. Touret, and S. Grinstein. The pH of the secretory pathway: measurement, determinants, and regulation. *Physiology* 19:207-215 (2004).
17. al-Awqati, Q. Chloride channels of intracellular organelles. *Curr. Opin. Cell Biol.* 7:504–508 (1995).
18. Tompkins, L.S., K.D. Nullmeyer, S.M. Murphy, C.S. Weber, and R.M. Lynch. Regulation of secretory granule pH in insulin-secreting cells. *Am. J. Physiol.* 283:C429–C437 (2002).
19. Eto, K., T. Yamashita, K. Hirose, Y. Tsubamoto, E.K. Ainscow, G.A. Rutter, S. Kimura, M. Noda, M. Iino, and T. Kadowaki. Glucose metabolism and glutamate analog acutely alkalinize pH of insulin secretory vesicles of pancreatic β-cells. *Am. J. Physiol.* 285:E262–E271 (2003).
20. Barg, S., P. Huang, L. Eliasson, D.J. Nelson, S. Obermuller, P. Rorsman, F. Thevenod, and E. Renstrom. Priming of insulin granules for exocytosis by granular Cl^- uptake and acidification. *J. Cell Sci.* 114, 2145–2154 (2001).
21. Decoursey, T.E. Voltage-gated proton channels and other proton transfer pathways. *Physiol. Rev.* 83:475-579 (2003).
22. Ramsey, I.S., E. Ruchti, J.S. Kaczmarek, and D.E. Clapham. Hv1 proton channels are required for high-level NADPH oxidase-dependent superoxide production during

thephagocyte respiratory burst. *Proc. Natl. Acad. Sci. U.S.A.* 106:7642-7647 (2009).

23. Wu, L.J., G. Wu, M.R.A. Sharif, A. Baker, Y. Jia, F.H. Fahey, H.R. Luo, E.P. Feener, and D.E. Clapham. The voltage-gated proton channel Hv1 enhances brain damage from ischemic stroke. *Nat. Neurosci.* 15:565-573 (2012).
24. Lishko, P.V., I.L. Botchkina, A. Fedorenko, and Y. Kirichok. Acid extrusion from human spermatozoa is mediated by flagellar voltage-gated proton channel. *Cell* 140: 327-337 (2010).
25. Wang, Y., S.J. Li, J. Pan, Y. Che, J. Yin, and Q. Zhao. Specific expression of the human voltage-gated proton channel Hv1 in highly metastatic breast cancer cells, promotes tumor progression and metastasis. *Biochem. Biophys. Res. Commun.* 412:353-359 (2011).
26. Wang, Y., S.J. Li, X. Wu, Y. Che, and Q. Li. Clinicopathological and Biological Significance of Human Voltage-gated Proton Channel Hv1 Protein Overexpression in Breast Cancer. *J. Biol. Chem.* 287:13877-13888 (2012).
27. Wang, Y., X. Wu, Q. Li, S. Zhang, and S.J. Li. Human Voltage-Gated Proton Channel Hv1: A New Potential Biomarker for Diagnosis and Prognosis of Colorectal Cancer. *PLoS One* 8:e70550 (2013).
28. Wang, Y., S. Zhang, and S.J. Li. Zn^{2+} induces apoptosis in human highly metastatic SHG-44 glioma cells, through inhibiting activity of the voltage-gated proton channel Hv1. *Biochem. Biophys. Res. Commun.* 438:312-317 (2013).
29. Ramsey, I.S., M.M. Moran, J.A. Chong, and D.E. Clapham. A voltage-gated proton-selective channel lacking the pore domain. *Nature* 440:1213-1216 (2006).
30. Sasaki, M., M. Takagi, and Y. Okamura. A voltage sensor-domain protein is a voltage-gated proton channel. *Science* 312:589-592 (2006).
31. Tombola, F., M.H. Ulbrich, and E.Y. Isacoff. The voltage-gated proton channel Hv1 has two pores, each controlled by one voltage sensor. *Neuron* 58, 546-556 (2008).
32. Li, S.J., Q. Zhao, Q. Zhou, H. Unno, Y. Zhai, and F. Sun. The role and structure of the carboxyl-terminal domain of the human voltage-gated proton channel Hv1. *J. Biol. Chem.* 285:12047-12054 (2010).

33. Musset, B., S.M.E. Smith, S. Rajan, V.V. Cherny, S. Sujai, D. Morgan, and T.E. DeCoursey. Zinc inhibition of monomeric and dimeric proton channels suggests cooperative gating. *J. Physiol.* 588:1435-1449 (2010).

34. Zhao, Q., Y. Che, Q. Li, S. Zhang, Y.T. Gao, Y. Wang, X. Wang, W. Xi, W. Zuo, and S.J. Li. The voltage-gated proton channel Hv1 is expressed in pancreatic islet β-cells and regulates insulin secretion. *Biochem. Biophys. Res. Commun.* 468:746-751 (2015).

35. Okochi, Y., Sasaki, M., Iwasaki, H., and Okamura, Y. Voltage-gated proton channel is expressed on phagosomes. *Biochem. Biophys. Res. Commun.* 382:274-279 (2009).

36. Lacy, P.E., and Kostianovsky, M. Method for the isolation of intact islets of Langerhans from the rat pancreas. *Diabetes* 16:35-39 (1967).

37. Renström, E., Eliasson, L., Bokvist, K., and Rorsman, P. Cooling inhibits exocytosis in single mouse pancreatic B-cells by suppression of granule mobilization. *J. Physiol. (Lond.)* 494:41-52 (1996).

38. Weinhaus, A.J., Poronnik, P., Tuch, B.E., and Cook, D.I. Mechanisms of arginine-induced increase in cytosolic calcium concentration in the beta-cell line NIT-1. *Diabetologia* 40:374-382 (1997).

39. Prentki, M., and Matschinsky, F.M. Ca^{2+}, cAMP, and phospholipid-derived messengers in coupling mechanisms of insulin secretion. *Physiol. Rev.* 67:1185-1248 (1987).

40. Gromada, J., Brock, B., Schmitz, O., and Rorsman, P. Glucagon-like peptide-1: regulation of insulin secretion and therapeutic potential. *Basic. Clin. Pharmacol. Toxicol.* 95:252-262 (2004).

41. DeCoursey, T.E. Voltage-gated proton channels: what's next? *J. Physiol.* 586:5305-5324 (2008).

42. Zhang, C.Y., Parton, L.E., Ye, C.P., Krauss, S., Shen, R., Lin, C.T., Porco, J.A. Jr, Lowell, B.B. Genipin inhibits UCP2-mediated proton leak and acutely reverses obesity- and high glucose-induced beta cell dysfunction in isolated pancreatic islets. *Cell Metab.* 3:417-427 (2006).

43. Geng, X., Li, L., Watkins, S., Robbins, P. D., and Drain P. The insulin secretory granule

is the major site of K (ATP) channels of the endocrine pancreas. *Diabetes* 52:767-776 (2003).

44. Demaurex, N., Furuya, W., D'Souza, S., Bonifacino, J. S., and Grinstein, S. Mechanism of acidification of the trans-Golginetwork (TGN). In situ measurements of pH using retrieval of TGN38 and furin from the cell surface. *J. Biol. Chem.* 273:2044-2051 (1998).
45. Schapiro, F. B., and Grinstein, S. Determinants of the pH of the Golgi complex. *J. Biol. Chem.* 275:21025-21032 (2000).
46. Al-Awqati, Q. Proton-translocating ATPases. *Annu. Rev. Cell Biol.* 2:179-199 (1986).
47. Burgess, T.L., and Kelly, R.B. Constitutive and regulated secretion of proteins. *Annu. Rev. Cell Biol.* 3:243-293 (1987).
48. Barg, B., Ma, X., Eliasson, L., Galvanovskis, J., Göpel, S.O., Obermüller, S., Platzer, J., Renström, E., Trus, M., Atlas, D., Striessnig, J., and Rorsman, P. Fast exocytosis with few Ca^{2+} channels in insulin-secreting mouse pancreatic B cells. *Biophys. J.* 81:3308-3323 (2001).
49. Seino, S., Takahashi, H., Fujimoto, W., and Shibasaki1, T. Roles of cAMP signalling in insulin granule exocytosis. *Diabetes Obes Metab.* 11 (4):180-188 (2009)
50. McQuaid, T.S., Saleh, M.C., Joseph, J.W. Gyulkhandanyan, A., Manning-Fox, J.E., MacLellan, J.D., Wheeler, M.B., and Chan, C.B. cAMP-mediated signaling normalizes glucose-stimulated insulin secretion in uncoupling protein-2 overexpressing b-cells. *J. Endocrinol.* 190:669-680 (2006).
51. de Rooij, J., Zwartkruis, F. J., Verheijen, M. H. Cool RH, Nijman, S. M., Wittinghofer, A., and Bos, J.L. Epac is a Rap1 guanine-nucleotide-exchange factor directly activated by cyclic AMP. *Nature* 396:474-477 (1998).
52. Proks, P., Reimann, F., Green, N., Gribble, F., and Ashcroft, F. Sulfonylurea stimulation of insulin secretion. *Diabetes* 51 (Suppl 3):S368-376 (2002).
53. Matschinsky, F.M., Glaser, B., and Magnuson, M.A. Pancreatic beta-cell glucokinase: closing the gap between theoretical concepts and experimental realities. *Diabetes* 47:307-315 (1998).

54. Weir, G.C., and Bonner-Weir, S. Five stages of evolving beta-cell dysfunction during progression to diabetes. *Diabetes* 53 (Suppl 3):S16-S21 (2004).

FIGURE LEGENDS

FIGURE 1. Reduced insulin secretion of islets from Hv1-deficient mice.

A: Glucose-, sulfonylurea-, KCl- and L-arginine-induced insulin secretion from isolated islets of KO, heterozygous and WT mice (n = 8 per genotype). Data are means ± SEM. ***$p < 0.001$, heterozygous vs. corresponding WT; $^{###}p < 0.001$, KO vs. corresponding WT; $^{\&\&\&}p < 0.001$, Glc, Tol, Glb, KCl or Arg vs. Basal for WT. Basal, 2.8 mM glucose; Glc, 16.7 mM glucose; Tol, 200 μM tolbutamide; Glb, 1 μM glibenclamide; KCl, 60 mM KCl; Arg, 10 mM L-arginine.

B and C: Insulin (B) and proinsulin (C) contents at a basal condition (2.8 mM glucose) in isolated islets from KO , heterozygous and WT mice (n = 8 per genotype). Data are means ± SEM. **$p < 0.01$, ***$p < 0.001$, KO vs. corresponding WT.

D: Ratio of insulin to proinsulin content of isolated islets of KO, heterozygous and WT mice at a basal condition (n = 8 per genotype). Data are means ± SEM. NS (no significance), vs. WT.

E: Proinsulin secretion at 16.7 mM glucose from isolated islets of KO, heterozygous and WT mice (n = 8 per genotype). Data are mean ± SEM. ***$p < 0.001$, KO or heterozygous vs. WT.

F: Ratio of insulin to proinsulin secretion of isolated islets of KO, heterozygous and WT mice at 16.7 mM glucose (n = 8 per genotype). Data are means ± SEM. NS (no significance), vs. WT.

FIGURE 2. siRNA-mediated knockdown of Hv1 inhibits secretagogue-induced insulin secretion.

A: Glucose- and sulfonylurea-induced insulin secretion from INS-1 (832/13) cells transfected with scramble (control) or Hv1-targeting siRNA (siRNA) (n = 8 per condition). Data are mean ± SEM. **$p < 0.01$,***$p < 0.001$, vs. corresponding control; $^{###}p < 0.01$, vs.

control at basal.

B and C: Insulin (B) and proinsulin (C) contents in the cells transfected with scramble (control) or Hv1-targeting siRNA (siRNA) at a basal condition (n = 8 per condition). Data are mean ± SEM. ***$p < 0.001$, vs. corresponding control.

D: The ratio of insulin to proinsulin content of the cells transfected with scramble (control) or Hv1-targeting siRNA (siRNA) at a basal condition (n = 8 per condition). Data are mean ± SEM. NS (no significance), vs. control.

E and F: Quantitative RT-PCR for insulin from INS-1 (832/13) cells (E) and isolated islets (F) treated with scramble (control) or Hv1-targeting siRNA (siRNA). Data are mean ± SEM (n = 3 per condition). *$p < 0.05$, vs. corresponding control.

G and H: Proinsulin secretion (G) and the ratio of insulin to proinsulin secretion (H) of INS-1 (832/13) cells transfected with scramble (control) or Hv1-targeting siRNA (siRNA) in the presence of 16.7 mM glucose. Data are mean ± SEM (n = 8 per condition). **$p <$ 0.01, ***$p < 0.001$, NS (no significance), vs. corresponding control. These data suggests that no significant accumulation of proinsulin occurred in KO islets.

FIGURE 3. Hv1-deficient mice exhibit hyperglycaemia and impaired glucose tolerance with reduced insulin secretion.

A: Body weight change of KO, heterozygous and WT mice ($n^{+/+} = 24$; $n^{+/-} = 24$; $n^{-/-} = 24$). Data are mean ± SEM.

B: Basal blood glucose concentrations after fasting 6 h in 4 month-old KO, heterozygous and WT mice ($n^{+/+} = 24$; $n^{+/-} = 24$; $n^{-/-} = 24$). Data are mean ± SEM. ***$p < 0.001$, KO or heterozygous vs. WT.

C: Blood glucose levels measured in whole blood following i.p. injection of glucose (2 g/kg body weight) in KO, heterozygous and WT mice ($n^{+/+} = 12$; $n^{+/-} = 12$; $n^{-/-} = 12$). Data are means ± SEM. *$p < 0.05$, ***$p < 0.001$, KO vs. WT.

D: Insulin concentrations measured in sera of KO, heterozygous and WT mice following i.p. glucose challenge (2 g/kg body weight) ($n^{+/+} = 8$; $n^{+/-} = 8$; $n^{-/-} = 8$). Data are means ± SEM. *$p < 0.05$, ***$p < 0.001$, KO vs. WT. Hv1KO mice exhibit a loss of acute phase insulin

secretion in response to glucose.

E: Insulin concentrations measured in sera of KO, heterozygous and WT mice following i.p. L-arginine challenge (1 g/kg body weight) ($n^{+/+}$ = 8; $n^{+/-}$ = 8; $n^{-/-}$ = 8). Data are means ± SEM. *p < 0.05, **p < 0.01, KO vs. WT. Hv1KO mice show a markedly decreased arginine-stimulated insulin secretion, but retaining first-phase secretion.

F: Blood glucose levels measured in whole blood following i.p. insulin injection (1 U/kg body weight) in KO, heterozygous and WT mice ($n^{+/+}$ = 12; $n^{+/-}$ = 12; $n^{-/-}$ = 12). Data are means ± SEM.

FIGURE 4. Deficiency of Hv1 has no effect on cAMP generation.

A: Insulin secretion of isolated islets transfected with scramble (control) or Hv1-targeting siRNA (siRNA) at 2.8 mM glucose, 2.8 mM glucose containing 10 μM forskolin, and 16.7 mM glucose containing 10 μM forskolin (n = 8 per condition). Data are mean ± SEM. *p < 0.05, **p < 0.01, ***p < 0.001, vs. corresponding control; $^{\#\#}p$ < 0.01, $^{\#\#\#}p$ < 0.001, vs. control at 2.8 mM glucose.

B: cAMP content of isolated islets transfected with scramble (control) or Hv1-targeting siRNA (siRNA) at 16.7 mM glucose containing 10 μM forskolin (n = 6 per condition). Data are mean ± SEM. NS (no significance), vs. control.

C: Insulin secretion of INS-1 (832/13) cells transfected with scramble (control) or Hv1-targeting siRNA (siRNA) at 16.7 mM glucose and in the presence of 10 or 100 nM GLP-1 (n = 6 per condition). Data are mean ± SEM. ***p < 0.001, vs. corresponding control; $^{\#\#\#}p$ < 0.001, vs. control without GLP-1.

FIGURE 5. Deficiency of Hv1 impairs cellular Ca^{2+} homeostasis and membrane depolarization, acidifies intragranules and alkalizes cytosol.

A, B and C: Knockdown of Hv1 impairs cellular Ca^{2+} homeostasis in INS-1 (832/13) cells. Cellular Ca^{2+} levels in INS-1 (832/13) cells were measured by Fura-2 fluorescence. The cells treated with scramble siRNA (control) or Hv1-targeting siRNA (siRNA) were kept at 2.8 mM glucose before switching to stimulation by 200 μM tolbutamide without (A) or

with (B) 16.7 mM glucose as indicated above the traces. The cells were kept at 2.8 mM glucose before switching to stimulation by 200 μM tolbutamide without or with 10 μM $ZnCl_2$ as indicated above the traces (C). This result indicates that Zn^{2+}, a classical inhibitor of Hv1 (29,41), can efficiently inhibit Ca^{2+} influx in the cells.

D and E: Knockdown of Hv1 impairs membrane depolarization induced by glucose or tolbutamide in INS-1 (832/13) cells. The membrane potential changes of INS-1 (832/13) cells during glucose- and tolbutamide-stimulation were monitored by $DiBAC_4(3)$ fluorescence. INS-1 (832/13) cells treated with scramble siRNA (control) or Hv1-targeting siRNA (siRNA) were kept at 2.8 mM glucose before switching to stimulation by 16.7 mM glucose (G) or 200 μM tolbutamide (H) as indicated above the traces.

F and G: Knockdown of Hv1 acidifies intragranules and alkalizes cytosol.

INS-1 (832/13) cells treated with scramble (control) or Hv1-targeting siRNA (siRNA) were loaded with fluorescent probe LSG (F) or BCECF-AM (G). The change of intragranule pH was estimated by the fluorescence intensity of LSG (F). The data were normalized to the control. Data are mean ± SEM (n = 5 per condition). $*p < 0.05$, vs. corresponding control.

FIGURE 6. Knockout of Hv1 decreases α and β cell masses.

A: Immunohistochemical analysis of 4 month-old WT, heterozygous and KO islets using anti-insulin and anti-glucagon antibodies. Representative images of H&E, anti-insulin and anti-glucagon antibody-stained pancreatic sections from 4 month-old WT, heterozygous and KO mice. Scale bar, 50 μm.

B and C: Relative islet number based on immunohistochemical analysis of pancreatic sections (B) and islet size calculated by isolated islet area (C) in 4 month-old WT and Hv1KO mice (n = 6 per genotype). Data are mean ± SEM. NS (no significance), $*p < 0.05$, vs. WT.

D: Relative islet area of 4 month-old WT and KO mice analyzed by immunohistochemistry of pancreatic sections (n = 6 per genotype). Data are mean ± SEM. $*p < 0.05$, vs. WT.

E and F: α and β cell masses of 4 month-old WT and KO mice based on immunostaining of pancreatic sections (n = 6 per genotype). Relative α and β cell masses were determined as a

ratio of total glucagon (α cell)- or insulin (β cell)-positive area to total pancreatic area. Twenty to thirty sections per pancreas were analyzed. Data are presented as mean ± SEM. *$p < 0.05$, **$p < 0.01$, vs. corresponding WT.

G: Pancreatic insulin content (n = 6 per genotype). Data are mean ± SEM. *$p < 0.05$, vs. WT.

FIGURE 7. Hv1-deficient mice exhibits an age-dependent development in glucose intolerance and a decrease in β cell mass.

A: Blood glucose levels measured in whole blood following i.p. injection of glucose (2 g/kg body weight) in 2 and 6 month-old KO and WT mice ($n^{+/+} = 11$; $n^{-/-} = 12$). Data are mean ± SEM. **$p < 0.01$, 2 vs. 6 month-old KO. The 6 month-old KO mice show more serious glucose intolerance than the 2 month-old KO mice.

B: Insulin concentrations measured in sera of 2 and 6 month-old KO and WT mice following i.p. glucose challenge (2 g/kg body weight) ($n^{+/+} = 10$; $n^{-/-} = 12$). Data are means ± SEM.

C: Insulin concentrations measured in sera of 2 and 6 month-old KO and WT mice following i.p. L-arginine challenge (1 g/kg body weight) ($n^{+/+} = 8$; $n^{-/-} = 8$). Data are means ± SEM.

D: Blood glucose levels measured in whole blood following i.p. insulin injection (1 U/kg body weight) in KO and WT mice ($n^{+/+} = 12$; $n^{+/-} = 12$; $n^{-/-} = 12$). Data are means ± SEM.

E: β cell masses of 2 and 6 month-old WT and KO mice based on immunostaining of pancreatic sections (n = 8 per genotype). Relative β cell masses were determined as a ratio of total insulin (β cell)-positive area to total pancreatic area. Twenty to thirty sections per pancreas were analyzed. Data are presented as mean ± SEM. *$p < 0.05$, KO vs. corresponding WT.

FIGURE 8. Effect of Hv1 on STZ-induced diabetes model.

A: Basal blood glucose concentrations after fasting 6 h in STZ-treated KO and WT mice ($n^{+/+} = 23$; $n^{-/-} = 27$). Data are mean ± SEM. *$p < 0.05$, KO vs. WT. AUC, area under the

curve.

B: Blood glucose levels measured in whole blood following i.p. injection of glucose (2 g/kg body weight) in STZ-treated KO and WT mice ($n^{+/+}$ = 12; $n^{-/-}$ = 14). Data are means ± SEM. *p < 0.05, KO vs. WT. AUC, area under the curve.

C: Insulin contents at a basal condition (2.8 mM glucose) in islets isolated from control and STZ-treated WT mice (n = 10 per genotype). Data are means ± SEM. ***p < 0.001, STZ vs. control.

D: 16.7 mM glucose-induced insulin secretion of islets isolated from control and STZ-treated WT mice (n = 8 per genotype). Data are means ± SEM. ***p < 0.001, STZ vs. control.

E: Immunohistochemical analysis of pancreas from mice treated with STZ (b and d) or saline (a and c, control) using anti-Hv1 and anti-insulin monoclonal antibodies. Representative images of anti-Hv1 (a, b) and anti-insulin (c, d) antibody-stained pancreatic sections. Scale bar, 50 μm. Mean optic density of Hv1- and insulin-positive area of islets of control and STZ-treated WT mice (e, Hv1, up panel; f, insulin, down panel). Twenty to thirty sections per pancreas were analyzed (n = 8 per condition). Data are means ± SEM. *p < 0.05, ***p < 0.001, STZ vs. control. Hv1 is down-regulated in pancreatic β cells in STZ-induced diabetic mice.

FIGURE 9. Hv1 is down-regulated in high glucose-induced dysfunctional β cells.

A: Glucose-induced insulin secretion from INS-1 (832/13) cells chronically incubated at 11 (control) and 25 mM (HG) glucose for 48 h. Data are mean ± SEM (n = 8 per condition). ***p < 0.001, vs. control.

B: Immunofluorescence analysis of INS-1 (832/13) cells chronically incubated at 11 (control) and 25 mM (HG) glucose for 48 h using anti-Hv1 monoclonal antibody. Representative images of anti-Hv1 monoclonal antibody-stained INS-1 (832/13) cells (a and c) and DAPI stain to visualize the nuclei (b and d). Scale bar, 20 μm. Mean fluorescence intensity of Hv1-positive area of the cells (e), expressed as an average of five experiments (Five different perspectives were counted per experiment. 50-150 cells per

perspective). Data are means ± SEM. ***$p < 0.001$, HG vs. control. Hv1 is also obviously down-regulated in dysfunctional INS-1 (832/13) cells.

Fig. 1

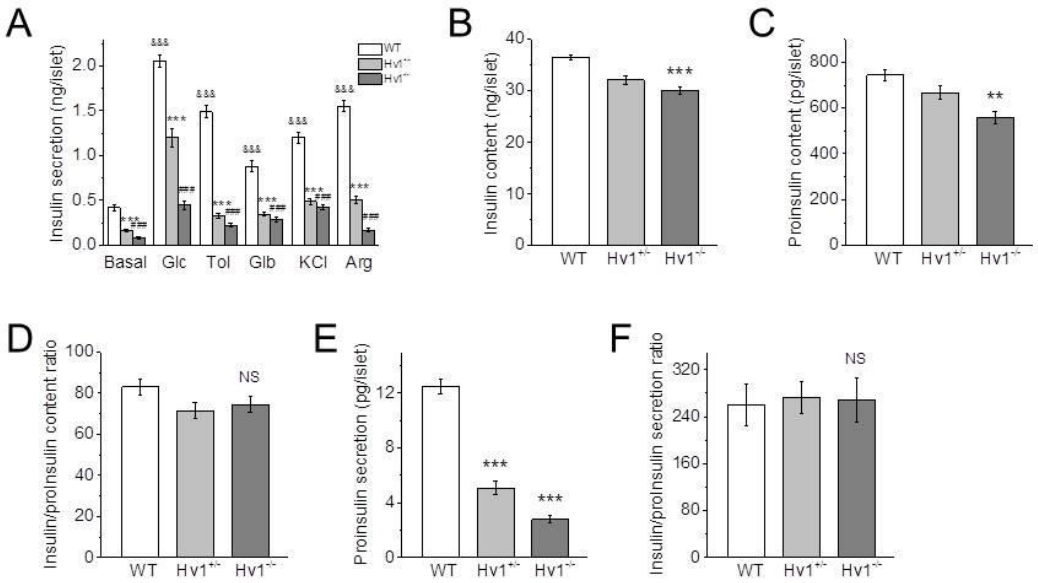
A
Insulin secretion (ng/islet)
WT
Hv1+/-
Hv1-/-
Basal
Glc
Tol
Glb
KCl
Arg
B
Insulin content (ng/islet)
C
Proinsulin content (pg/islet)
D
Insulin/proInsulin content ratio
NS
E
Proinsulin secretion (pg/islet)
F
Insulin/proInsulin secretion ratio
NS

Fig. 2

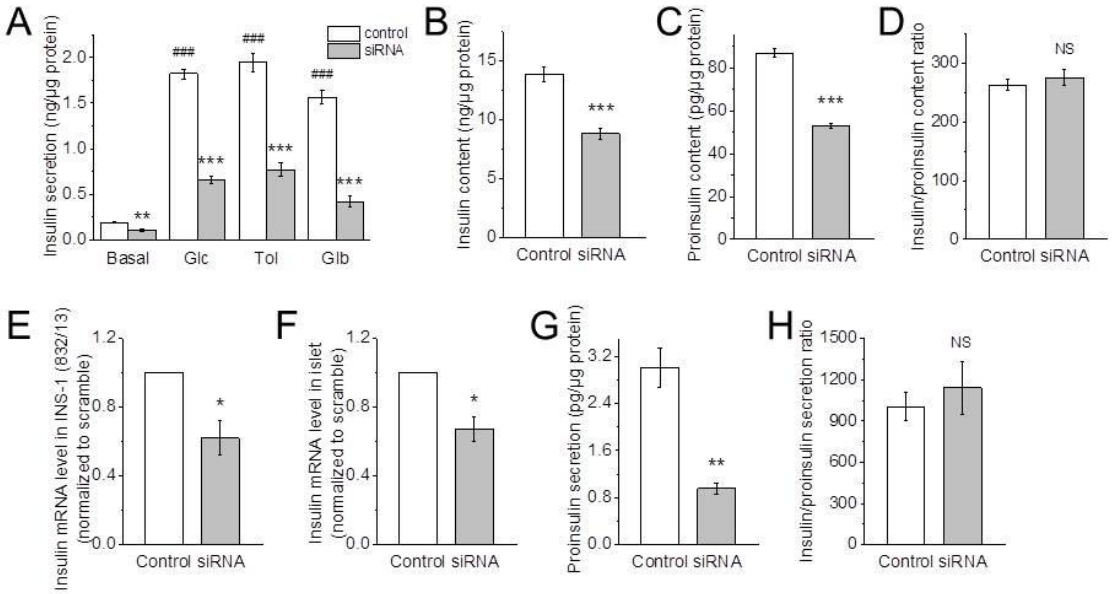
A
Insulin secretion (ng/μg protein)
control
siRNA
###
***
**
Basal
Glc
Tol
Glb
B
Insulin content (ng/μg protein)
***
Control siRNA
C
Proinsulin content (pg/μg protein)
***
Control siRNA
D
Insulin/proinsulin content ratio
NS
Control siRNA
E
Insulin mRNA level in INS-1 (832/13) (normalized to scramble)
*
Control siRNA
F
Insulin mRNA level in islet (normalized to scramble)
*
Control siRNA
G
Proinsulin secretion (pg/μg protein)
**
Control siRNA
H
Insulin/proinsulin secretion ratio
NS
Control siRNA

Fig. 3

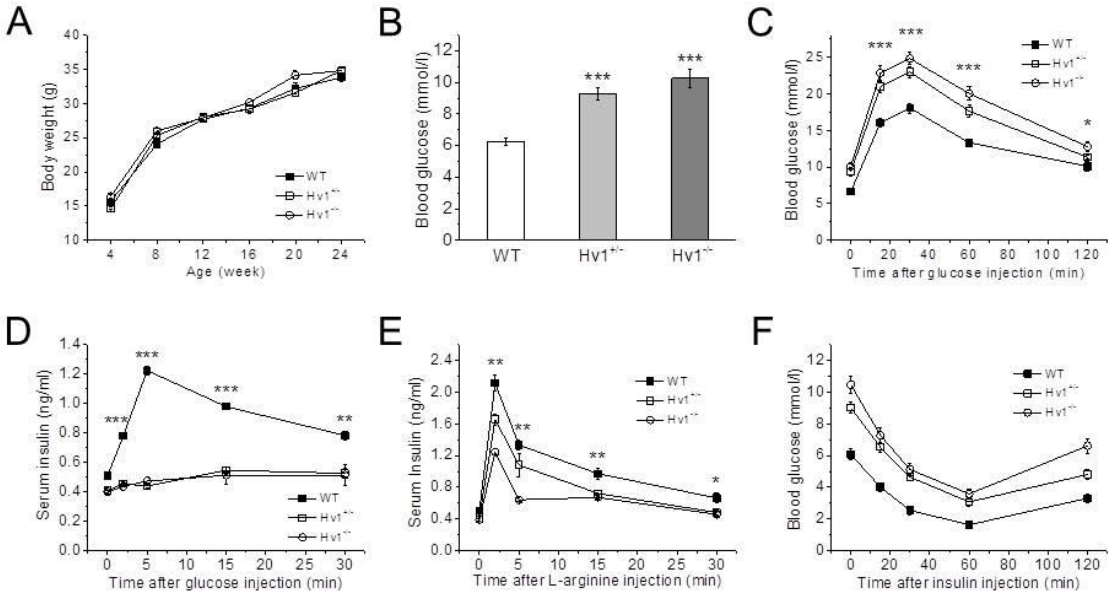
A
Body weight (g)
Age (week)
WT
Hv1+/-
Hv1-/-
B
Blood glucose (mmol/l)
WT
Hv1+/-
Hv1-/-
C
Blood glucose (mmol/l)
Time after glucose injection (min)
D
Serum insulin (ng/ml)
Time after glucose injection (min)
E
Serum Insulin (ng/ml)
Time after L-arginine injection (min)
F
Blood glucose (mmol/l)
Time after insulin injection (min)

Fig. 4

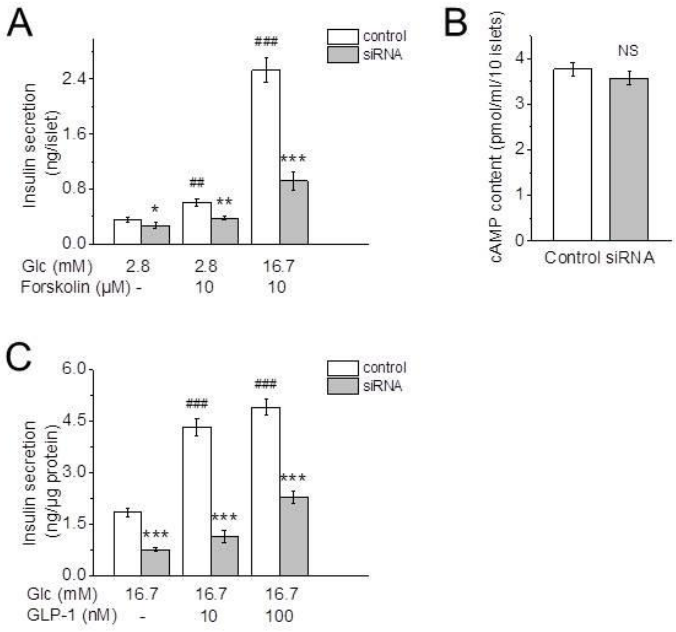
A
control
siRNA
Insulin secretion (ng/islet)
0.0
0.8
1.6
2.4
###
##
*
**
***
Glc (mM) 2.8 2.8 16.7
Forskolin (μM) - 10 10
B
cAMP content (pmol/ml/10 islets)
0
1
2
3
4
NS
Control siRNA
C
control
siRNA
Insulin secretion (ng/μg protein)
0.0
1.5
3.0
4.5
6.0
###
###
***
***
***
Glc (mM) 16.7 16.7 16.7
GLP-1 (nM) - 10 100

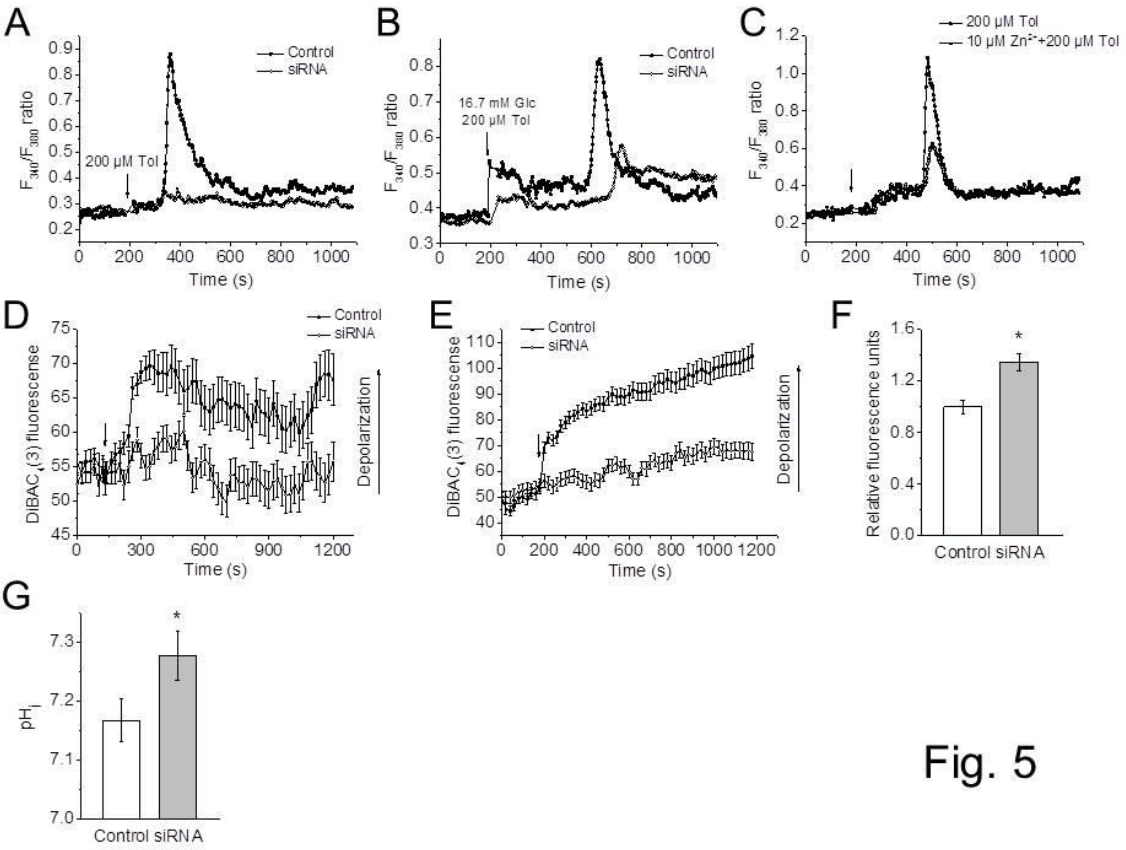
A
Control
siRNA
200 μM Tol
F_{340}/F_{380} ratio
Time (s)
B
Control
siRNA
16.7 mM Glc
200 μM Tol
F_{340}/F_{380} ratio
Time (s)
C
200 μM Tol
10 μM Zn^{2+}+200 μM Tol
F_{340}/F_{380} ratio
Time (s)
D
Control
siRNA
$DiBAC_4(3)$ fluorescense
Depolarization
Time (s)
E
Control
siRNA
$DiBAC_4(3)$ fluorescense
Depolarization
Time (s)
F
Relative fluorescence units
Control siRNA
G
pH_i
Control siRNA

Fig. 5

Fig. 6

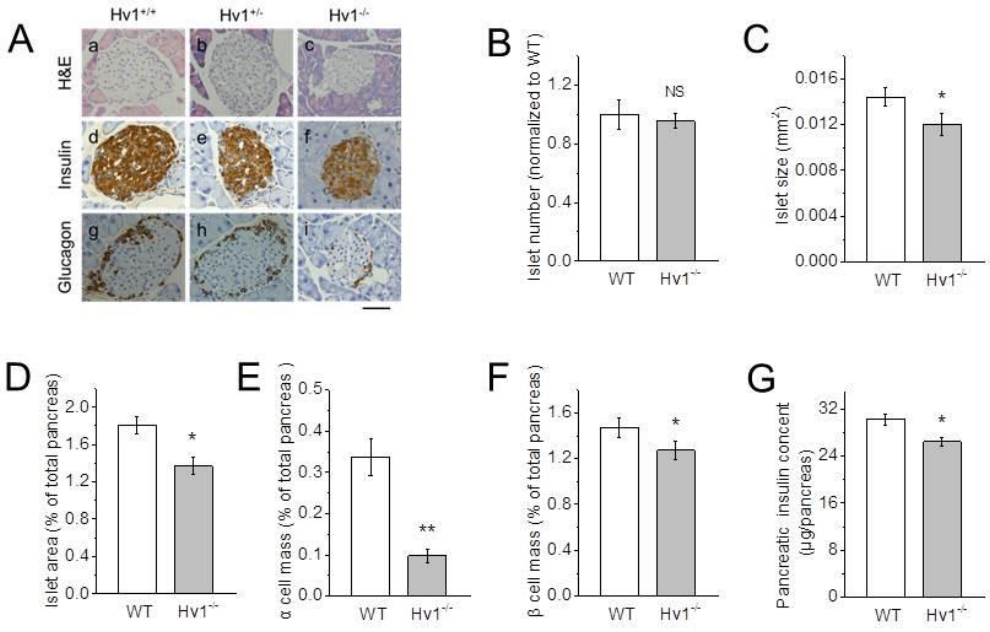
A
Hv1+/+
Hv1+/-
Hv1-/-
H&E
Insulin
Glucagon
a
b
c
d
e
f
g
h
i
B
Islet number (normalized to WT)
NS
WT
Hv1-/-
C
Islet size (mm-2)
*
D
Islet area (% of total pancreas)
E
α cell mass (% of total pancreas)
**
F
β cell mass (% of total pancreas)
G
Pancreatic insulin concent (μg/pancreas)

Fig. 7

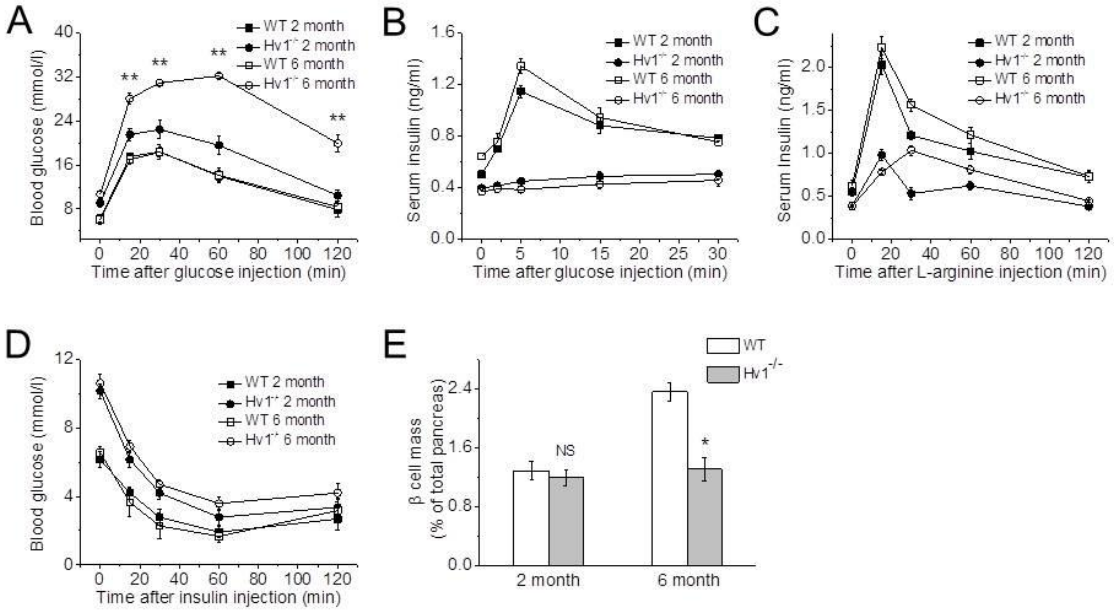
A
Blood glucose (mmol/l)
Time after glucose injection (min)
WT 2 month
Hv1-/- 2 month
WT 6 month
Hv1-/- 6 month
**
B
Serum insulin (ng/ml)
Time after glucose injection (min)
C
Serum Insulin (ng/ml)
Time after L-arginine injection (min)
D
Blood glucose (mmol/l)
Time after insulin injection (min)
E
β cell mass (% of total pancreas)
WT
Hv1-/-
NS
*
2 month
6 month

Fig. 8

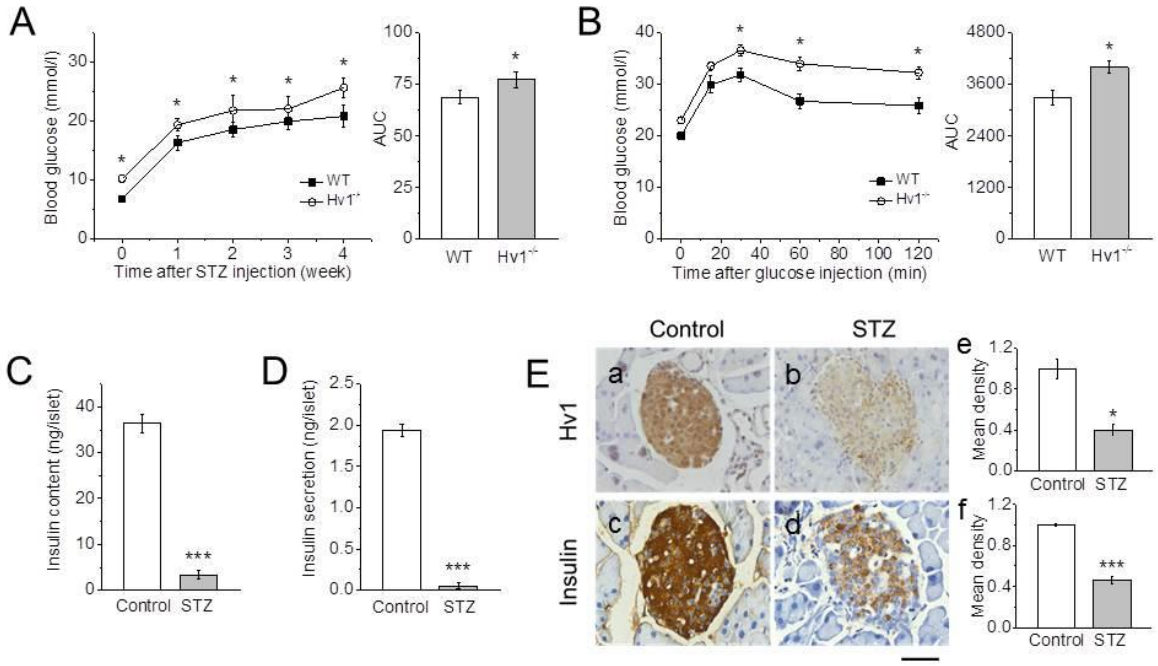
A
Blood glucose (mmol/l)
Time after STZ injection (week)
WT
Hv1-/-
AUC
B
Blood glucose (mmol/l)
Time after glucose injection (min)
C
Insulin content (ng/islet)
Control
STZ
D
Insulin secretion (ng/islet)
E
Control
STZ
Hv1
Insulin
a
b
c
d
e
Mean density
f

Fig. 9

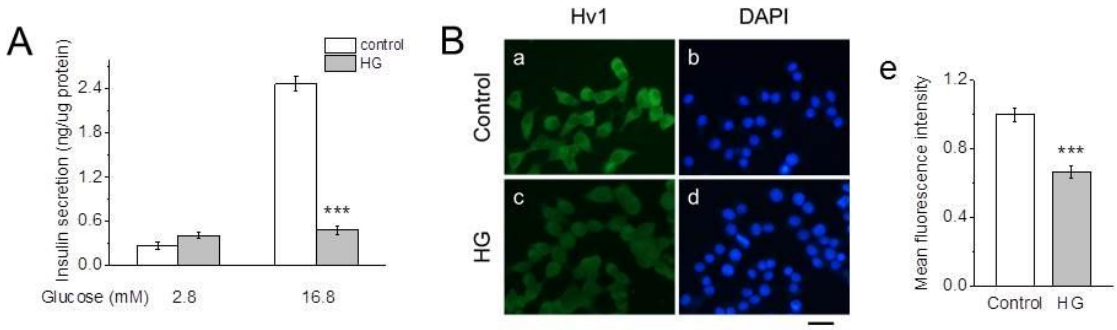
A
control
HG
Insulin secretion (ng/ug protein)
2.4
1.8
1.2
0.6
0.0
***
Glucose (mM)
2.8
16.8
B
Hv1
DAPI
Control
HG
a
b
c
d
e
Mean fluorescence intensity
1.2
0.8
0.4
0.0
***
Control
HG